

Research Article

Enhanced PV Network Controller for Optimizing Performance of LFC Power Systems

Zainab Ali Abboud^{1,*,} ¹ *Electrical Engineering Technology Dept, Engineering Technical College, Al-Esraa University, Baghdad, Iraq.*

ARTICLE INFO

Article History

Received 24 Oct 2024

Revised: 29 Nov 2024

Accepted 18 Dec 2024

Published 10 Jan 2025

Keywords

Renewable Power ,

Heliacal ,

Wind ,

Photovoltaic ,

Green Power ,

Load Frequency Control,

Control grid



ABSTRACT

Turkey has made national energy accessibility the top of its priorities. Less than 90% of the nation's 82 million citizens can access electricity today. Workers use solar power and wind energy to provide more electricity across the nation. Solar power wind power and power electronics help Turkey save money as it works to fix its energy issues. Load Frequency Control inverters help Turkey as a developing country reduce solar power costs through advanced power electronics technologies. IC-based electronics improvements let us make energy components work better at less cost compared to previous expensive hardware. LFC inverters help add renewable energy to existing grids according to latest research and can solve energy problems worldwide. The analysis sees solar power providing 35% of Turkey's power output by 2050. Wind energy stands out for its unmatched marginal fuel cost advantage. Utility-scale solar power beats other generation sources because it costs no fuel to produce power while releasing minimal greenhouse gases which supports global decarbonization efforts. The analysis shows that our updated energy model matches actual LFC metering data through similar energy output numbers and trends. Our predicted numbers using the standard Load Flow Control system proved less precise than actual measurements. Our simulation produced 3.9% additional renewable energy estimates than actual meter readings whereas the basic model showed 52% less output. Our revised energy model in MATLAB shows good precision when it uses 10% solar power and 9.90% wind power input. Our hybrid scheme produced precise predictions when combining both solar and wind systems with 57.16% solar and 57.20% wind percentages.

1. INTRODUCTION

Organizations must buy solar power generation kits to help customers use this energy source. Nonprofit Independent System Operators established by FERC maintain a primary role in this process. As power system regulators ISOs control how energy moves through grids while maintaining fair power system markets and managing purchased power agreements to design energy systems that meet customer needs. ISOs maintain their operational expenses through small service fees collected from everyone who buys and sells energy. These organizations manage electricity supply and demand for more than 60 percent of our national markets. Generators who take part in the market system place offers against each other to sell electricity and win available supply options.

In America solar power now supplies 4.5% of all electricity generation with market experts estimating it will reach 35% by 2050. Normal operations of solar energy systems cost less because they use no additional fuel like what power plants burn. Research in [1] shows solar technology plays a crucial role in creating a clean power network and meeting climate goals because it generates almost zero pollution and uses scarce resources to produce electricity.

Power produced by different arrays enters the system by following a cost-based scheduling process which matches power demands with available generation sources from lowest to highest costs. Inside the energy power grids of region ISOs the solar energy flows through to supply homes and businesses [2]. Solar energy integration into electricity market competition delivers lower wholesale electricity prices that help consumers. The factors contributing to reduced solar generation costs include:

- The volume of solar energy supplied to the market,
- The level of demand, and
- The marginal cost and availability of other market inputs.

*Corresponding author. Email: zainababboud@esraa.edu.iq

A model examining the market mechanism, based on historical market data, estimates the price changes resulting from increased solar penetration. Assuming short-term demand inelasticity and excluding the long-term effects of market exit by competing firms, the analysis reveals a significant impact on next-day electricity markets, which currently account for 30–40% of power purchases in a region serving 14 million people, as detailed in [3].

2. LITERATURE REVIEW

The complete computational system for structural power design includes many settings that create a challenging modeling environment. Several researchers tried to make power simulation modeling easier through analysis of parameter effects. The extensive time it takes to build valid energy models hinders widespread adoption in engineering organizations but is cited by [4] as their main discovery. A detailed study of how input variables affect output results helps speed up and refine the modeling process for renewable energy systems. As [5] explains accurate estimates need high precision but straightforward measurements that perform well in real-world environments are just as necessary. Research from [6] shows that a small number of input parameters significantly affect power consumption outcomes and need specific examination. The article [7] shows how researchers now study sensitivity and uncertainty analysis more often with building models including retrofit projects.

Research into renewable energy modeling already exists yet studies still lack methods to measure the effect of solar power production on electricity prices when modeling future energy changes with historical data. This research first examines solar pricing and energy mix structures before detailing how to better model energy market supply and demand. This evaluation also studies the design limitations that reduce how much prices drop.

Research into solar power explains how it affects electricity prices both positively and negatively depending on market conditions. Research teams have used worldwide market data to investigate the effects of solar and other renewable power generation on electricity prices. Research studies show that renewable energy spot prices react to solar power output in markets where solar accounts for 20% of total generation capacity [8]. When solar power generation reaches high levels the average market price for solar energy decreases substantially until spot prices drop to zero during 2% of times when solar energy supplies 40% of the total electricity generation. Studies in references [9] and [10] find that merit-order pricing leads to zero or negative prices at times because of power plant mix changes and conventional generator operation limits. Researchers study Italian electricity markets by creating models that examine wind and power market reactions to price reductions while accounting for demand levels and fuel expenses.

The power of solar energy to reshape electric rates depends on several key aspects including solar ratio levels plus how well utilities predict future demand plus what rules control power markets. Research in [11] discovered that more solar power integration creates bigger swings in power market prices especially during shorter trading intervals. The prices of generated power depend on the energy supply and demand for each area. Turkey uses imported electricity at 48% of its energy mix so adding more solar power capacity does not affect normal electricity rates [12]. When solar penetration levels are high gas and oil generation sources typically become less needed according to [13]. When solar predictions show less accuracy the power supply system depends more heavily on gas and oil as backup resources.

Structural market models continue to be used because they correctly display current market conditions between suppliers and customers. The study by reference [14] enhanced structural models through hockey-stick curves to compute price spikes and temperature-responsive demand parameters. The study of [15] showed how natural gas and electricity prices connect in Mid-Atlantic power markets through detailed market response models.

Solar and wind power integration requires engineering solutions according to the research presented in [16]. The heavy on-and-off cycles of baseload plants used to compensate for unreliable renewable power leads to added upkeep expenses and failures that reduce fuel savings. The effect of solar power appears mostly in capacity markets but these results form the basis of thorough solar energy impact research. The study from [17] shows wind power affects power lines minimally at low solar penetration yet the effects could grow at higher levels of solar integration.

The results of energy simulations depend heavily on specific data about heat settings plus device and lighting use practices. The study results demonstrated how building occupant activities shape these key variables most strongly in offices and homes. High ventilation rates must run through fume hoods and to meet clean air standards for industrial settings. Our analysis will improve energy simulation results by making changes to temperature setpoints plus setting lighting equipment schedules occupancy plans and ventilation levels [18-25].

3. METHODOLOGY

The research part of this document studies Photovoltaic (PV) systems and Load Frequency Control (LFC) which produce sustainable renewable energy. The section first explains how researchers executed their simulation process for every case study creating an organized way to study the data. The chapter explains the main use of MATLAB simulation software. The segment below offers the basics of PV systems and Load Frequency Control then sets standard criteria for checking energy

model accuracy. This chapter reviews what specific factors affected the study results and explains all design adjustments made.

3.1 Calculating The PV and LFC For Generating Power

Pertaining the LFC for generating the renewable energy.

$$CSP(t) = R_i(t) + Ld_i(t) = +v_c(t) \quad (1)$$

$$\frac{d_i(t)}{dt} = -\frac{R_i(t)}{L} - \frac{v_c(t)}{L} + \frac{v_i(t)}{L} \quad (2)$$

The generation across the whole generating process is given by -

$$v_c(t) = \frac{1}{c} \int i(t) dt \quad (3)$$

The LFC equation considered together with respect to time.

$$\frac{dv_c(t)}{dt} = \frac{i(t)}{c} \quad (4)$$

$$\text{State vector}, X = \begin{bmatrix} v(t) \\ v_c(t) \end{bmatrix} \quad (5)$$

$$\text{Differential State Vector}, X = \begin{bmatrix} \frac{di(t)}{dt} \\ \frac{dv_c(t)}{dt} \end{bmatrix} \quad (6)$$

$$X = \begin{bmatrix} \frac{di(t)}{dt} \\ \frac{dv_c(t)}{dt} \end{bmatrix} = \begin{bmatrix} -\frac{R}{L} & -\frac{1}{L} \\ \frac{1}{c} & 0 \end{bmatrix} \begin{bmatrix} i(t) \\ v_c(t) \end{bmatrix} + \begin{bmatrix} \frac{1}{L} \\ 0 \end{bmatrix} [v_i(t)] \quad (7)$$

$$Y = [0 \quad 1] \begin{bmatrix} i(t) \\ v_c(t) \end{bmatrix} \quad (8)$$

Where,

$$A = \begin{bmatrix} -\frac{R}{L} & -\frac{1}{L} \\ \frac{1}{c} & 0 \end{bmatrix} B = \begin{bmatrix} \frac{1}{L} \\ 0 \end{bmatrix} C = [0 \quad 1] \text{ and } D = [0] \quad (9)$$

Hybrid PV as well as LFC Style Equation:

$$CSP = \frac{b_0}{s^n + U_1(t) - 1s^{n-1} + \dots + k_1 s + U_1(t)} \quad (10)$$

Repositioning the above equation as

$$(s^n + U_1(t)s^{n-1} + \dots + a_0 B(s) = b_0 M(s)) \quad (11)$$

On both sides of the hybrid PV and LFC equation model, apply the inverse Laplace transform.

$$\frac{d^n y(t)}{dt^n} + k_{n-1} \frac{d^{n-1} y(t)}{dt^{n-1}} + \dots + k \frac{dy(t)}{dt} + k_0 y(t) = b_0 u(t) \quad (12)$$

Let

$$\begin{aligned} y(t) &= x_1 \\ \frac{dy(t)}{dt} &= x_2 = x_1 \\ \frac{d^2 y(t)}{dt^2} &= x_3 = x_2 \end{aligned}$$

$$\begin{aligned}\frac{d^{n-1}y(t)}{dt^{n-1}} &= x_n = x'_{n-1} \\ \frac{d^n y(t)}{dt^n} &= x'_n \\ \text{And } u(t) &= u\end{aligned}$$

Then, the generic equation for PV and LFC deduced for supply/demand in MATLAB Simulation is given by:

$$x k'_{n-1} + kx_n + \dots + k_1 x_2 + kx_1 = B_0 U_1(t) \quad (13)$$

Rewriting the above equation as given by.

$$x k'_{n-1} = -k_0 x_1 - k_1 x_2 - \dots - k_{n-1} x_n + B_0 U_1(t) \quad (14)$$

The output equation is given by:

$$y(t) = y = x_1 \quad (15)$$

The hybrid model becomes –

$$\begin{aligned}X^i &= \begin{bmatrix} x^i_1 \\ x^i_2 \\ \vdots \\ x^i_{n-1} \\ x^i_n \end{bmatrix} \\ &= \begin{bmatrix} \begin{bmatrix} 0 & 1 & 0 \\ 0 & 0 & 1 \\ \vdots & \vdots & \vdots \\ 0 & 0 & 0 \\ -a_0 & -a_1 & -a_2 \end{bmatrix} \dots \begin{bmatrix} 0 & 0 \\ 0 & 0 \\ \vdots & \vdots \\ 0 & 1 \\ -a_{n-2} & -a_{n-1} \end{bmatrix} \begin{bmatrix} x_1 \\ x_2 \\ \vdots \\ x_{n-1} \\ x_n \end{bmatrix} + \begin{bmatrix} 0 \\ 0 \\ \vdots \\ 0 \\ b_0 \end{bmatrix} \end{bmatrix} [u] \quad (16)\end{aligned}$$

$$\begin{aligned}PV &= [1 \quad 0 \quad \dots \quad 0 \quad 0] \begin{bmatrix} X_1 \\ X_2 \\ \vdots \\ x_{n-1} \\ x_n \end{bmatrix} \\ \text{Here } D &= (0) \quad (17)\end{aligned}$$

Renewable Energy Calculation Equation:

$$R.E: \frac{dx}{dy} = f(x, y) y(0) = y_0 \quad (18)$$

$$\frac{y(s)}{u(s)} = \frac{1}{s^2 + s + 1} \quad (19)$$

Reposition of the renewable energy order equation is given as:

$$(s^2 + s + 1)Y(s) = U(s) \quad (20)$$

Pertaining inverse Laplace transform on both the sides.

$$\frac{d^2 y(t)}{dt^2} + \frac{dy(t)}{dt} + y(t) = u(t) \quad (21)$$

Let

$$\begin{aligned}y(t) &= x_1 \\ \frac{dy(t)}{dt} &= x_2 = x_1' \\ \text{And } u(t) &= u\end{aligned}$$

Then, the basic LFC and PV state equation is

$$\dot{x}_2 = -x_1 - x_2 + u \quad (22)$$

The output equation is

$$y(t) = y = x_1 \quad (23)$$

Repositioning the above equation as follow

$$(s^n + a_{n-1}s^{n-1} + \dots + a_1s + a_0)v(s) = u(s) \quad (24)$$

Substituting the inverse Laplace transform on both the sides.

$$\frac{d^n v(t)}{dt^n} + a_{n-1} \frac{d^{n-1} v(t)}{dt^{n-1}} + \dots + a_1 \frac{dv(t)}{dt} + a_0 v(t) = u(t) \quad (25)$$

Let

$$\begin{aligned} v(t) &= x_1 \\ \frac{dv(t)}{dt} &= x_2 = \dot{x}_1 \\ \frac{d^2 v(t)}{dt^2} &= x_3 = \dot{x}_2 \\ \frac{d^{n-1} v(t)}{dt^{n-1}} &= x_n = \dot{x}_{n-1} \\ \frac{d^n v(t)}{dt^n} &= \dot{x}_n \\ \text{And } u(t) &= u \end{aligned}$$

Considering the comparison between 2 set of results as follow:

$$\frac{y(s)}{v(s)} = b_n s^n + b_{n-1} s^{n-1} + \dots + b_1 s + b_0 \quad (26)$$

Repositioning the above equation as follow:

$$PV(s) = (b_n s^n + b_{n-1} s^{n-1} + \dots + b_1 s + b_0)v(s) \quad (27)$$

Applying the inverse Laplace transform to both sides facilitates the calculation of the Root Mean Square Error (RMSE) for the Load Frequency Control (LFC) and Photovoltaic (PV) systems.

$$CSP(t) = b_n \frac{d^n v(t)}{dt^n} + b_{n-1} \frac{d^{n-1} v(t)}{dt^{n-1}} + \dots + b_1 \frac{dv(t)}{dt} + b_0 v(t) \quad (28)$$

Bids go through an allocation process that generates an exponential supply curve until its price matches market demand at a specific point. This section analyzes how supply curve characteristics and demand patterns combine to determine the market results. Our simple diagram shows how supply and demand interact.

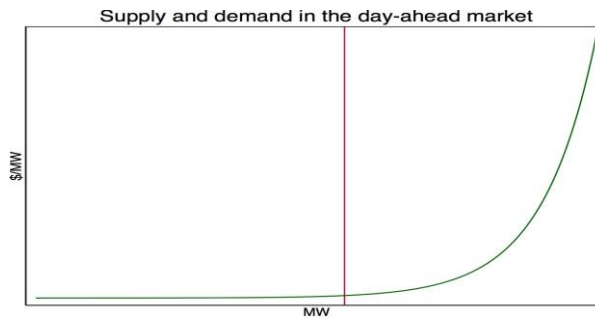


Fig. 1. A diagram illustrating the correlation between supply and demand.

3.2 Analyzing the PV and LFC Demand

The impact of demand on price is evident: When demand grows the clearing price goes up the same amount. Heating and cooling appliances drives regular changes in how much people need electricity and what rate providers charge them as summer turns to winter. Demand levels go up and down daily with matching trends across different seasons. During summer

the highest power usage occurs at 3 PM when customers turn on cooling units against the day's extreme heat. During most seasons demand spikes twice a day when people begin or end their daily routines. Although summer dominates other seasons with total demand the highest it sees in the mid-afternoon this time leads winter with its higher usage because of reduced daylight and more indoor time. Spring and fall display similar demand patterns. The lowest demand happens early in the morning and through the nighttime when most people stay in bed.

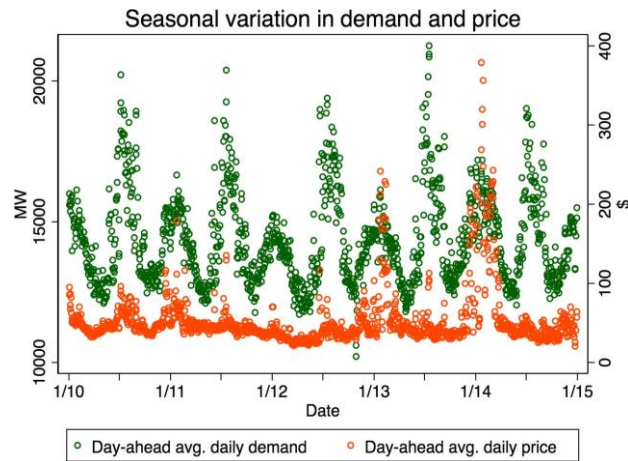


Fig. 3. A depiction of the concurrent spikes in demand and price.

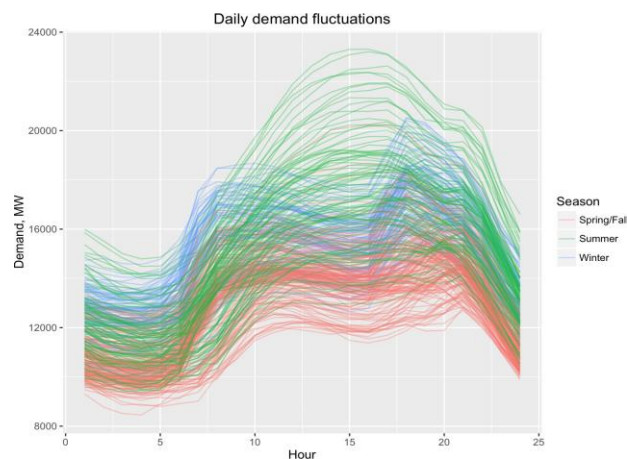


Fig. 4. Seasonal variations in daily demand patterns.

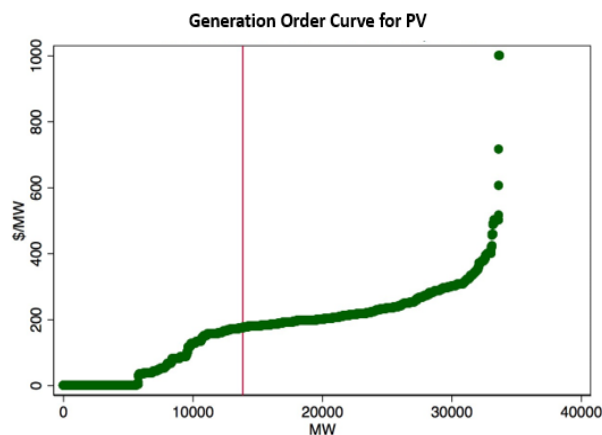


Fig. 5. The exponential structure of the bidding curve for photovoltaic (PV) generation.

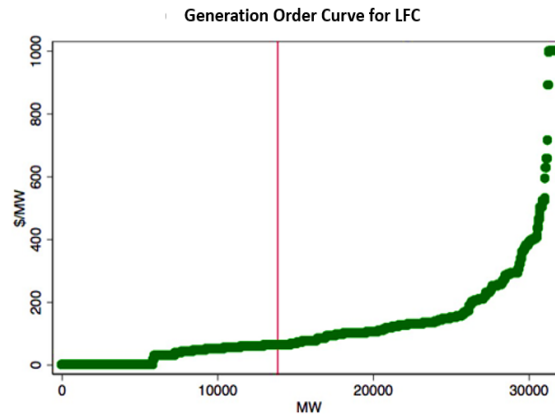


Fig. 6. The use of marginal costs to determine the slope of the bid curve for Load Frequency Control (LFC) generation.

3.3 Interaction OF PV-LFC Supply and Demand

The different curves show how energy mix strongly impacts final pricing results. The slopes of the supply curve establish market prices and stability through a certain relationship with each individual demand point. With demand held constant, two primary changes in the supply curve can lead to an increase in the clearing price: The price of generation resources falls when new power plants enter the market before demand levels. Forward prices rise when existing plants boost their rates or leave the market from these positions. How does the market respond when new generation resources appear to the left of demand? When other generation resources fall below market-clearing rates. Solar energy bidding at zero dollars drives competitors' market bids higher in the second case scenario.

Changes in demand make it difficult to tell if price effects result from shifting supply curves or changes to the market equilibrium point. For increased power generation to result in a lower clearing price, the following conditions must be met: Without affecting generator rates to the left of customer demand areas and forcing generator removals from the grid solar energy must still operate. Load Frequency Control ensures market fairness so the stated conditions should not be broken.

Any impact seen can exist only because of inherent power plant attributes that make their price drop below market value or force them to stop operating. The examination avoids confusion by recognizing distinct factors that influence neither solar power generation nor these outcomes independently. When temperatures drop people use more gas for heating which drives up gas prices and solar generation rises at the same time. Regular solar generation operations do not establish a direct influence on other power sources. The method presumes that raising power levels through generation won't directly influence how other production sources operate.

3.4 Accuracy Benchmark for Load Frequency Control

Micro-Grid systems need to be installed to measure how parameter changes affect power simulations while creating dependable system protocols. Our analysis uses statistical formulas to develop methods that calculate uncertainty in microgrid simulation models. Since none of the research-built energy models demanded precision calibration to particular structures the accuracy assessment follows established industry standards. We use the Root Mean Square Error (RMSE) standard to measure model accuracy by finding the differences between projective energy consumption and actual monthly results.

3.5 Changing Parameters for Load Frequency Control

Our research tests different input specifications from published sources to improve simulation precision. The essential simulation data consists of equipment operational and occupancy schedules plus detailed information about electrical loads and air vents plus air conditioning and ambient temperature parameters. We based our updates on the Micro-Grid Standard and Load Frequency Control requirements plus Photovoltaic technical specs and Simulation Century suggestions.

3.6 Temperature and Humidity Set-Points

How high and low hospitals set their building temperature controls affects their power usage significantly. These areas need tight control over temperature and humidity standards. The Load Frequency Control rules for setting temperatures and humidity defined how these areas should function. The LFC requirements demand constant temperature and humidity controls in hospital building generation spaces because these sensitive spaces need exact environmental balance. Gracile climate zones let staff adjust temperature and humidity to better fit workplaces and classroom settings. The program adjusts its environmental controls according to unique performance standards that vary across functional areas.

TABLE I. THE LFC DESIGN MANUAL SPECIFIES THE FOLLOWING

Time	Heat degree °F (°C)	Humidity Relative (HRH %)
Summertime	73 Plus/Minus 2 (23 Plus/Minus 1)	50 Plus/Minus 5
Wintertime	70 Plus/Minus 2 (21 Plus/Minus 1)	33 Plus/Minus 5

TABLE II. PROGRAM ASSUMPTIONS FOR TEMPERATURE AS WELL AS HUMIDITY LEVELS UTILIZED AT SEATS OTHER THAN EXPERIMENTATIONS.

Time / Fixed point	Fixed point Heat degree °F / °C	Setback Heat degree °F / °C	Humidity Relative (HRH%)
Summertime	75 °F / 24°C	82 °F / 28 °C	10 to 90
Wintertime	68 °F / 20 °C	50 °F / 10 °C	10 to 90

3.7 Real Renewable Energy Data On Load Frequency Control

Because solar energy bidders set their prices at \$0.00 or less they trigger a rightward movement in the bidding curve that matches the quantity of available solar production. When suppliers bid with prices of zero they effectively wipe out the demand from market price determination. Assuming new solar bids leave other bidders unchanged they will reliably lower market prices.

When forced market exits create supply adjustments in the power generation sector our final power mix would change. The impact of generator exits remains uncertain due to poor availability of exit patterns information. The impact of adding 5,000 MW of solar power generates to the system shows up as distance between the two curves where they intersect the demand line.

4. RESULTS

When forecasted solar power increases they often decrease their own bid offering levels to create higher electricity prices. The behavior shows as a downward trend between solar power production and total non-solar production. I check for this connection by analyzing the daily solar power output against total available solar generation above zero.

The dataset cannot tell us which generators supply energy beyond solar power so we use non-zero price bids as our indicator. Our method leaves out both renewable power sources that bid like solar and nuclear facilities that offer generation at no price. At prices close to solar power prices there is no reason for resources to behave strategically because market conditions push them towards price-taking behavior. Our study found no link between solar generation levels and strategic withdrawal behavior as the data results show no significant impact.

Our simulation considers solar power bids without any cost as our standard input. Even though solar bids at extremely low negative prices as long as these bids do not drive power prices below zero. Most price variations come from when generators with higher prices on the right side of the bidding curve need to make room for new participants. The clearing price change depends on two factors: Generator positioning on the bid curve determines both prices shifts at the curve edge and generator price differences near the marginal provider.

Since the effects of wholesale market price changes on residential electricity rates remain unclear our simulation treats electricity demand as unresponsive to price changes. About 65% of global electricity prices comes from buying energy on the wholesale market with distribution and transmission handling the remaining 35%. Since perfect inelasticity does not apply to real-world demand this model assumption allows us to simplify the simulation process and account for actual pricing results.

Based on present information all power supplies except these generators hold their real prices stable which unrealistic over time. Growing solar energy access will drive out older inexpensive generators located at the bottom end of bids from operation. Generator exit depends on their success in day-ahead commodities markets as well as capacity market earnings. Our ability to predict these impacts stays restricted due to insufficient data on generator withdrawal patterns and reasons. The implications of this assumption are uncertain: Market prices could rise when higher demand situations push generators below solar plants to exit from electricity markets. Generator exits at the top echelon of the curve that rarely operate cause no major changes in market prices throughout demand ranges.

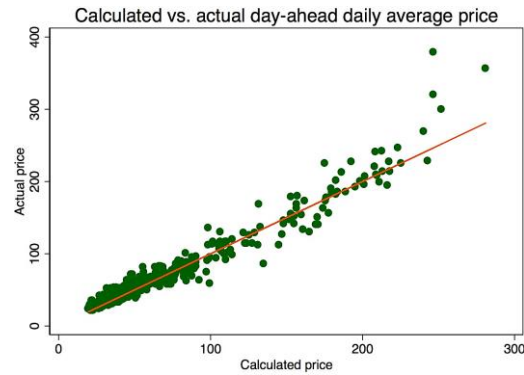


Fig. 7. The greatest discrepancies between calculated and actual prices occur during price spikes. The orange line represents a one-to-one relationship.

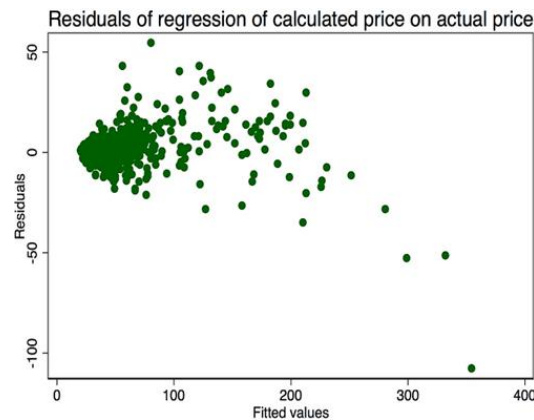


Fig. 8. As actual prices increase, calculated prices tend to skew lower.

The turbines of solar energy systems run directly from sunlight making them free from fuel costs. Despite solar power system maintenance and operation expenses its energy costs compare favorably against coal, natural gas, hydropower, and nuclear power sources. Our updated power model tracks real energy usage patterns based on actual Load Frequency Control readings from the power grid. Unlike the default model which displayed extreme error rates the actual LFC data showed through an underestimation of renewable energy production by over 53%. After changing the inputs we increased renewable energy uptake by 4% yet our improved model predicted 11.5% from solar and 10.66% from wind power use. Compared to other models the hybrid PV-LFC model generated 58.1% solar power along with 56.10% wind energy as shown by renewable energy indexes tracking.

Our analysis shows heavyweight price swings depend on hourly customer demands and power plant selection patterns. The addition of power plants at times with high electricity need creates sharper price drops due to the featured price structure that grows exponentially. Installed solar panels follow a vertical mirror image of merit order up to total demand point. The visual charts that follow show this pattern.

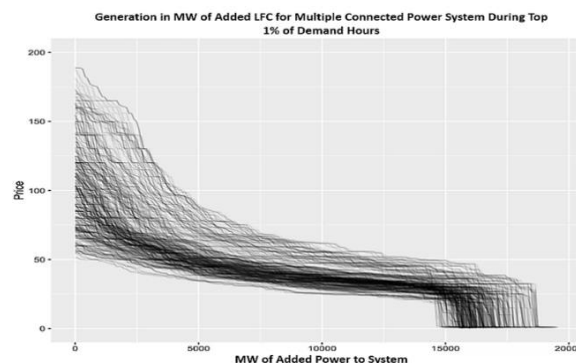


Fig. 9. During high-demand hours, prices drop sharply as additional megawatts are added to the system.

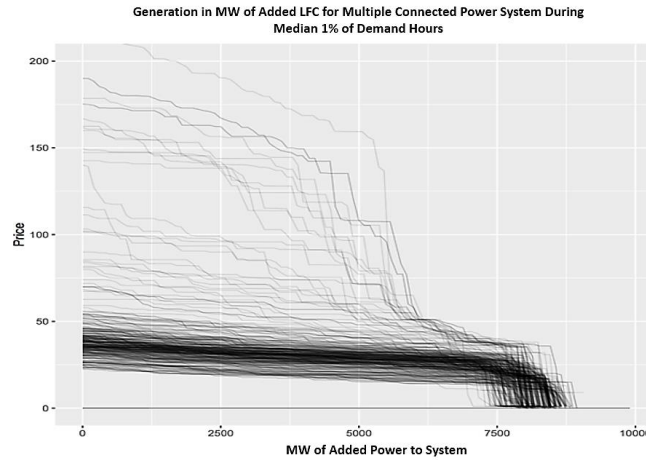


Fig. 10. The curve's gradual upward slope mirrors the center of the bid curve, dominated by power generation sources with similar pricing.

To study Turkey's future energy system this evaluation examines how wind and solar power affect energy prices across consumption groups and the share of natural gas in total generation.

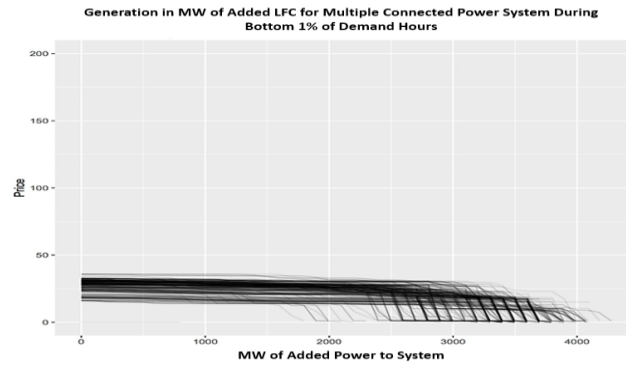


Fig. 11. At low demand levels, increased electricity generation results in stable prices.

The market impact that added generation produces should reflect expected price patterns in power today. When mid-tier generators leave instead of price-clearing plant operators the benefits of price reduction expected from expanded generation won't emerge. Our analysis continues to hold true because we base our findings on generators at the margin who need to exit first under our assumptions.

A significant shift in consumer response may develop because lowering prices through generation changes can trigger future demand growth. The rise in electric vehicle usage will create much bigger growth compared to this effect. The amount of energy a power system receives from new generation sources varies depending on weather changes particularly for solar power technology.

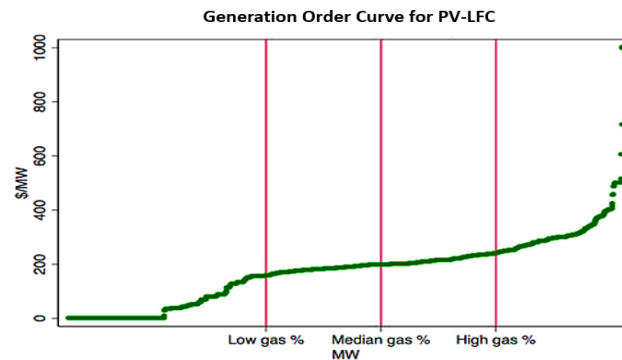


Fig. 12. This graph illustrates the varying contributions of PV-LFC generation to grid supply at different demand levels.

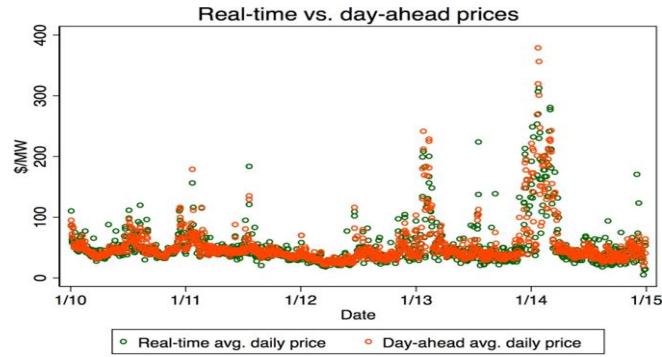


Fig. 13. A close relationship exists between real-time and day-ahead energy costs, with real-time prices exhibiting a slightly higher standard deviation (34.217 vs. 33.717 for day-ahead).

5. DISCUSSIONS

The cost of losses at a specific node (location) on the grid, Differences between actual electrical system cost and typical market node valuations expose ways power grids operate less effectively. Strained power grids require operators to select expensive generators from lower priority positions to meet system requirements. When temperature deviates greatly from its typical 50°F value it tends to lessen the price differences between system nodes.

Findings show that the cost of grid congestion does not contribute statistically to the overall price changes. The connection between simulation forecasts and actual power system pricing stays strong through all scenarios examined. The regression analysis shows that the relationship between simulated prices and actual data aligns perfectly except at higher price points.

TABLE III. ACCURACY MEASUREMENTS FOR DEFAULT AND CUSTOMIZED ENERGY MODELS ACROSS VARIOUS POWER SOURCES, DETAILING PERCENTAGES FOR RENEWABLE ENERGY GENERATION AND TOTAL POWER GENERATION.

State-research	Overall Generation (%)	Phase	Simulation-Default		Simulation-Modified	
Photovoltaic (PV)	31%	New Construction	Renewable	heliacal= 27.1% Wind= 27.8%	Renewable	heliacal= 11.2% Wind= 10.0%
Load Frequency Control (LFC)	55%	Before Renewable energy renovation	Renewable	heliacal= 57.2% Wind= 57.2%	Renewable	heliacal= 10.9% Wind=9.9%
			Renewable	Temperature =83.2% Temperature = 64.5%	Renewable	Temperature = 33.9% Temperature = 27.3%
			Renewable	heliacal =45.6% Wind=45.0%	Renewable	heliacal =8.1% Wind=7.9%
			Renewable	Temperature =86.2% Temperature =64.3%	Renewable	Temperature =31.2% Temperature =23.3%
		After Renewable energy renovation	Thermic	heliacal= 11.7% Wind= 10.5%	Thermic	heliacal= 13.2% Wind= 11.1%
			Thermic	heliacal= 14.4% Wind= 13.4%	Thermic	heliacal= 12.2% Wind=11.0%
Onshore-Offshore	22%					

A generation space area percentage affects how much renewable energy a certain area produces. Renewing multiple zones throughout the building did not damage its core construction elements. Power production and delivery activities demonstrated the strongest influence on energy results because these operations use large amounts of energy and maintain critical temperatures. The marginal loss component shows how much transmission and reserve reserve issues increase the costs of completing energy operations according to merit order rules. The system does not include this piece in its wholesale energy pricing calculations.

TABLE IV. REGRESSION ANALYSIS OF THE RESOURCE MIX AND ITS INFLUENCE ON PRICE.

Sources	(1)
	Average
% Coal	2.827*** (16.52)
% Hydro	-0.436
	(-1.66)
% Nuclear	-0.199
	(-1.78)
% Oil	10.41*** (35.29)
% Refuse	-1.795
	(-1.54)
% Solar	-2.657
	(-0.40)
% Wind	1.117
	(1.64)
Day-ahead demand avg.	0.000869
	(1.53)
Constant	35.46** (2.74)
Observations	1260
<i>t</i> statistics in parentheses	

6. CONCLUSION

Our research brings Photovoltaic systems and Load Frequency Control controllers together to create micro-grids inside LFC-equipped modern buildings. Our research demonstrates how switching to powerful energy systems helps reduce costs and educates controller teams about what PV and LFC integration has achieved. Building this culture now gives our green energy team at PV and LFC full authority to suggest additional power system enhancements. The PV and LFC controller staff should ask the green team's help when making plans for power system facility projects. Greater use of solar power can make a big financial impact on the system since it creates only 5.4% of electricity generation now while forecasted to reach 40% by 2050. Solar power operates without material fuel expenses while matching costs with existing energy types like coal nuclear and hydropower. Our enhanced model shows realistic renewable energy numbers where solar supplies 11.5% power and wind generates 10.66%. Our hybrid PV-LFC system provides stronger output results compared to separate systems with PV delivering 58.12% and Wind supplying 56.10%. Our results show that combining PV and LFC systems can improve how today's power grids work both effectively and sustainably.

Conflicts of Interest

The author's disclosure statement confirms the absence of any conflicts of interest.

Funding

No grant or sponsorship is mentioned in the paper, suggesting that the author received no financial assistance.

Acknowledgment

The author extends appreciation to the institution for their unwavering support and encouragement during the course of this research.

References

- [1] R.Frunzulica, A.Damian, M.S.Toropoc, and A.N.Sandu, "Aspects on modeling and sizing a cogeneration/trigeneration source for a hospital building," in Proc. 2019 Int. Conf. ENERGY and ENVIRONMENT (CIEM), Timisoara, Romania, 17–18 Oct. 2019, pp. 500–504.
- [2] S. G. Sigarchian, A. Malmquist, and V. Martin, "Design optimization of a complex polygeneration system for a hospital," *Energies*, vol. 11, no. 5, p. 1071, 2018.
- [3] N. M. Isa, H. S. Das, C. W. Tan, A. Yatim, and K. Y. Lau, "A techno-economic assessment of a combined heat and power photovoltaic/fuel cell/battery energy system in Malaysia hospital," *Energy*, vol. 112, pp. 75–90, 2016.
- [4] Y. Shu, K. Ito, and R. Yokoyama, "Sensitivity analysis in structure optimization of energy supply systems for a hospital," *Energy Convers. Manage.*, vol. 48, no. 8, pp. 2836–2843, 2017.
- [5] L. Schweber, "The effect of BREEAM on clients and construction professionals," *Build. Res. Inf.*, vol. 41, no. 2, pp. 129–145, 2013.

- [6] L. Schweber and H. Haroglu, "Comparing the fit between BREEAM assessment and design processes," *Build. Res. Inf.*, vol. 42, no. 3, pp. 300–317, 2014.
- [7] Y. Alhor, M. Arif, T. Bano, C. Egbu, A. Mazroei, and E. Elsarrag, "Creating a better healing environment in Qatari healthcare sector: Exploring the research agenda for the future," *Int. J. Sustain. Built Environ.*, vol. 4, no. 2, pp. 158–164, 2015.
- [8] J. Ferreira, M. D. Pinheiro, and J. D. Brito, "Portuguese sustainable construction assessment tools benchmarked with BREEAM and LEED: An energy analysis," *Energy Build.*, vol. 69, pp. 451–463, 2014.
- [9] P. Wu, Y. Song, W. Shou, H. Chi, H. Y. Chong, and M. Sutrisna, "A comprehensive analysis of the credits obtained by LEED 2019 certified green buildings," *Renew. Sustain. Energy Rev.*, vol. 68, pp. 370–379, 2017.
- [10] S. Azhar, W. A. Carlton, D. Olsen, and I. Ahmad, "Building information modeling for sustainable design and LEED rating analysis," *Autom. Constr.*, vol. 20, no. 2, pp. 217–224, 2011.
- [11] R. Pradinuk, "Incentivizing the Daylit Hospital: The Green Guide for Health Care Approach," *HERD Health Environ. Res. Des. J.*, vol. 2, no. 2, pp. 92–112, 2009.
- [12] M. Younger, H. R. Morrow-Almeida, S. M. Vindigni, and A. L. Dannenberg, "The built environment, climate change, and health: Opportunities for co-benefits," *Am. J. Prev. Med.*, vol. 35, no. 5, pp. 517–526, 2018.
- [13] Y. Liu, X. Guo, and F. Hu, "Cost-benefit analysis on green building energy efficiency technology application: A case in China," *Energy Build.*, vol. 82, pp. 37–46, 2014.
- [14] Y. Zhang, J. Wang, F. Hu, and Y. Wang, "Comparison of evaluation standards for green building in China, Britain, United States," *Renew. Sustain. Energy Rev.*, vol. 68, pt. 1, pp. 262–271, 2017.
- [15] Z. Jian, S. Pullen, R. Rameezdeen, H. Bennetts, Y. Wang, G. Mao, Z. Zhou, H. Du, H. Duan, "Green building evaluation from a life-cycle perspective in Australia: A critical review," *Renew. Sustain. Energy Rev.*, vol. 70, pp. 358–368, 2017.
- [16] S. Chen, N. Li, J. Guan, Y. Xie, F. Sun, and J. Ni, "A statistical method to investigate national energy consumption in the residential building sector of China," *Energy Build.*, vol. 40, no. 4, pp. 654–665, 2008.
- [17] R. Benelmir and M. Feidt, "Energy cogeneration systems and energy management strategy," *Energy Convers. Manag.*, vol. 39, no. 10, pp. 1791–1802, 2018.
- [18] L. Vanhoutteghem, G. C. J. Skarning, C. A. Hviid, and S. Svendsen, "Impact of façade window design on energy, day lighting and thermal comfort in nearly zero-energy houses," *Energy Build.*, vol. 102, pp. 149–156, 2015.
- [19] F. R. D. A. Alfno, B. W. Olesen, B. I. Palella, and G. Riccio, "Thermal comfort: Design and assessment for energy saving," *Energy Build.*, vol. 81, pp. 326–336, 2014.
- [20] S. Del Ferraro, S. Iavicoli, S. Russo, and V. Molinaro, "A field study on thermal comfort in an Italian hospital considering differences in gender and age," *Appl. Ergon.*, vol. 50, pp. 177–184, 2015.
- [21] M. Golbazi and C. B. Aktas, "Analysis of credits earned by LEED healthcare certified facilities," *Procedia Eng.*, vol. 145, pp. 203–210, 2016.
- [22] J. Han, G. Zhang, Q. Zhang, J. Zhang, J. Liu, L. Tian, C. Zheng, J. Hao, J. Lin, Y. Liu, et al., "Field study on occupants' thermal comfort and residential thermal environment in a hot-humid climate of China," *Build. Environ.*, vol. 42, no. 12, pp. 4043–4050, 2017.
- [23] A. Pourshaghagh and M. Omidvari, "Examination of thermal comfort in a hospital using PMV-PPD model," *Appl. Ergon.*, vol. 43, no. 6, pp. 1089–1095, 2020.
- [24] S. Sattayakorn, M. Ichinose, and R. Sasaki, "Clarifying thermal comfort of healthcare occupants in tropical region: A case of indoor environment in Thai hospitals," *Energy Build.*, vol. 149, pp. 45–57, 2017.
- [25] J. Skoog, N. Fransson, and L. Jagemar, "Thermal environment in Swedish hospitals: Summer and winter measurements," *Energy Build.*, vol. 37, no. 9, pp. 872–877, 2015.